Applied Ocean Research 127 (2022) 103289

Contents lists available at ScienceDirect

Applied Ocean Research

journal homepage: www.elsevier.com/locate/apor

A WAVEWATCH III® model approach to investigating ocean wave source terms for West Africa: Non-linear wave-wave interaction source terms

Bennet Atsu Kwame Foli [a,b,*], Joseph K. Ansong [c], Kwasi Appeaning Addo [a,d], George Wiafe [a,b]

[a] Department of Marine and Fisheries Sciences, College of Basic and Applied Sciences, University of Ghana, P. O. Box LG99, Legon, Ghana
[b] Global Monitoring for Environment and Security and Africa, College of Basic and Applied Sciences, University of Ghana, c/o P. O. Box LG99, Legon, Ghana
[c] Department of Mathematics, University of Ghana, Legon, Ghana
[d] Institute of Environment and Sanitation Studies, University of Ghana, Legon, Ghana

ARTICLE INFO

Keywords:
Non-linear wave source term
Significant wave height
WAVEWATCH III
Wave direction
Wave forecasting
West Africa

ABSTRACT

Ocean wave forecasting for West Africa has mostly relied on global parameterization schemes and data outputs. Investigating non-linear ocean wave-wave interaction source terms (S_{nl}) for the region, that forms part of the wave model parameterization schemes, is a contribution of this study towards developing a regional wave modelling scheme for West Africa. The study evaluates five non-linear source term configurations with the WAVEWATCH III® (WW3) numerical ocean wave model version 5.16; (i) No source term applied - NL0, (ii) Discrete Interaction Approximation (DIA) – NL1, (iii) Exact Interaction Approximation – NL2, (iv) Generalized Multiple DIA – NL3, and (v) Two-Scale Approximation – NL4, in order to determine best performing S_{nl} for projecting significant wave heights and directions for the region. The wave simulations were run on three separate grids comprising a low resolution West Africa grid (latitudes 10° S – 30° N; longitudes 35° W – 15° E), high resolution south-eastern (latitudes 2° S – 8° N; longitudes 10° W – 10° E) and north-western (latitudes 10° N – 25° N; longitudes 30° W – 10° W) sub-grids. Simulations for the entire West Africa grid produced higher accuracies for the wave parameters compared to the higher resolution sub-grids. NL0 best estimates significant wave height whereas NL3 best estimates wave directions for the West Africa grid. For combined stations of the south-eastern sub-grid, while NL1 best estimates wave heights, NL3 best estimates the wave directions with possible alternation with NL1 due to insignificant differences. Similarly, for the north-western sub-grid, while NL1 best estimates significant wave heights, NL0 best estimates wave directions with similar ability to alternate with NL2 in projecting wave directions. Generally, insignificant differences exist between the source terms in projecting wave directions, especially for the north-western sub-region, implying that any of the source terms may be used in projecting wave directions without significantly compromising on accuracy. Thus, NL1 which best estimates significant wave heights for both south-eastern and north-western sub-regions can also be used in estimating the wave directions. Similarly, NL0 would be appropriate for the entire West Africa region.

1. Introduction

Ocean wave models have improved over the years. Wave models have progressed from first to third generation with the enhancement of computer technologies for faster and elaborate computations that enable larger data processing as well as real-time assimilations in ocean wave projections. Prediction of global ocean wave properties has been largely achieved and access to modelled ocean data has been made relatively easier. Nevertheless, the available global ocean wave data are based on global parameterization schemes, which can result in meso-scale regional and local phenomena being lost or undetected. It is therefore important that regional or local scale phenomena are studied using regionally or locally generated model outputs with corresponding parameterization schemes.

The prediction of ocean waves has been shown to rely on functions such as the input, dissipation, non-linear interaction, linear propagation, and bottom friction terms among others (Liu et al., 2017; van Vledder, 2006; Wang et al., 2017; WAVEWATCH III Development Group, 2016).

Abbreviations: WW3, WAVEWATCH III; S_{nl}, Non-linear wave-wave interaction source term; DIA, Discrete Interaction Approximation.

* Corresponding author at: Department of Marine and Fisheries Sciences, College of Basic and Applied Sciences, University of Ghana, P. O. Box LG99, Legon, Ghana.
E-mail address: bafoli@ug.edu.gh (B.A.K. Foli).

https://doi.org/10.1016/j.apor.2022.103289
Received 10 March 2022; Received in revised form 29 June 2022; Accepted 18 July 2022
Available online 11 August 2022

These functions cumulatively interplay to describe the behaviour of ocean waves, which is represented by stochastic mathematical relationships. Among the various source terms, the non-linear wave-wave interaction term plays a critical role in describing the evolution of wind generated waves (Gouin et al., 2016; Hasselmann et al., 1973; Polnikov, 2020; Tolman, 2004; Young and Van Vledder, 1993). Nonlinear wave interactions are a representation of how wave energy is shifted from higher to lower frequencies (Gouin et al., 2016; Hasselmann et al., 1973; Puscasu, 2014; Resio et al., 2001).

In the West Africa region, there is no established source term that describes the non-linear ocean wave-wave interaction behaviour. Since the inclusion of non-linear behaviour in ocean wave projection equations forms an integral part of ocean wave models, it is imperative that non-linear interaction term be investigated and appropriate ones established for the region in order to enhance accurate prediction. Thus, the aim of this study is to determine the appropriate non-linear wave-wave interaction source terms for accurate projections of ocean wave properties in the West Africa region. This study is a follow-up of Foli et al. (2022) in which we investigated the input and dissipation source terms.

1.1. Wave model theoretical background

Third generation ocean wave models evaluate the nonlinear source term (S_{nl}) explicitly without the presumption of a spectral shape (Ardhuin et al., 2010; Tolman, 2004). In the evolution of the spectrum of ocean wind-waves as described by Hasselmann (1960), a spectral balance equation as presented in (Eq. (1)) is used to describe the wave energy spectrum. The S_{tot} term in Eq. (1) is a representation of all cumulative sum of sources and sinks of energy to or from the spectral components of the resultant wave. Eq. (1) is the simplest representation of the wave balance equation (Fernández et al., 2021; Tolman, 2004; Tolman et al., 2002).

$$\frac{DF}{Dt} = S_{tot} = S_{in} + S_{nl} + S_{ds} \tag{1}$$

The spectral balance equation (Eq. (1)) comprise of an input source term as a result of wind (S_{in}), a non-linear wave-wave interaction term (S_{nl}) and a dissipation term (S_{ds}). According to Tolman (2004), these three terms are the elementary components of the wave spectral balance equation needed for estimating ocean wave properties. Other additional terms such as the linear propagation term (S_{ln}), bottom friction (S_{bot}) and reflection (S_{ref}), may only contribute to altering the energy. F in Eq. (1) describes the local wave energy spectrum.

The use of WW3 wave model on regional level has been established in previous studies (Fernández et al., 2021; Khan et al., 2021; Remya et al., 2020; Swain et al., 2019). WW3 is a 3rd generation wave model that incorporates several wave parameterization schemes that cover deep-ocean as well as coastal shallow water areas (Gouin et al., 2016; Resio et al., 2001; Tolman, 2013). As indicated by several studies (Fernández et al., 2021; Kalourazi et al., 2021; Swain et al., 2018; Tolman, 2013), WW3 operates on the spectral balance equation to estimate ocean wave properties. It also allows for an additional experimental source term (S_{xx}) as a user-defined term to Eq. (1) (WAVEWATCH III Development Group, 2016).

1.2. Non-linear wave-wave interaction source terms

This sub-section presents an abridged review of the presently available non-linear wave-wave interaction source terms implemented in the WW3 wave model. Different non-linear source terms, S_{nl}, are implemented in the WW3 wave model. The non-linear interaction source term was originally derived as a six-dimensional full Boltzmann integral (Tolman and Krasnopolsky, 2004; Tolman and Chalikov, 1996). However, the computational cost of implementing the full Boltzmann integral made it economically inefficient for operational use, and thus led to simpler modifications and more economically viable parameterisations. Within the WW3 model, S_{nl}, can be modelled using either the discrete interaction approximation (DIA), exact interaction approximation (WRT), Generalized Multiple DIA (GMD), or the two-scale approximation (TSA) parameterisations. The WW3 model also gives an option of implementation without a non-linear source term. In addition to the above mentioned non-linear source terms, there exist other non-linear parameterizations which include variants of the DIA such as the Fast DIA (FDIA; Polnikov, 2020), the simplified Research Institute for Applied Mechanics (SRIAM) (Komatsu and Masuda, 1996; Tamura et al., 2008), and the generalized kinetic equation of Gramstad and Babanin (2016) as presented in de León and Osborne (2020).

The framework for the computation of non-linear wave interactions was developed by Hasselmann (1962), which comprised the evaluation of a six-dimensional integral formulation known as the Boltzmann integral. According to Hasselmann (1962), there exist resonant non-linear interactions among four wave components (also referred to as quadruplets), where there is exchange of energy, momentum and action among the quadruplets. These four wave component quadruplets have wave number vectors represented by $\mathbf{k_1}$ through $\mathbf{k_4}$, and having corresponding radian frequencies σ_1 to σ_4. The conditions for the resonant non-linear interactions require that (Hasselmann, 1962, 1963a, 1963b):

$$\vec{k}_1 + \vec{k}_2 = \vec{k}_3 + \vec{k}_4, \tag{2}$$

and

$$\sigma_1 + \sigma_2 = \sigma_3 + \sigma_4 \tag{3}$$

The wave number k and the frequency σ, are said to satisfy the general wave dispersion relation:

$$\sigma^2 = gk\tanh kd \tag{4}$$

where g is gravitational acceleration and d is the mean water depth.

Hasselmann (1963a, 1963b) described the non-linear wave interactions among the quadruplets in terms of action densities n, with respect to the wave number vector $\boldsymbol{k}$, as the full Boltzmann integral for wind waves. This is represented by Eq. (5) (Hasselmann, 1963a, 1963b; van Vledder and Bottema, 2003):

$$\frac{\partial n_1}{\partial t} = \int\int\int G\left(\vec{k}_1, \vec{k}_2, \vec{k}_3, \vec{k}_4\right) \times \delta\left(\vec{k}_1 + \vec{k}_2 - \vec{k}_3 - \vec{k}_4\right) \times \delta(\sigma_1 + \sigma_2 - \sigma_3 - \sigma_4) \times [n_1 n_2 (n_3 + n_4) - (n_1 + n_2) n_3 n_4] d\vec{k}_2 d\vec{k}_3 d\vec{k}_4, \tag{5}$$

where $n_i = n(\boldsymbol{k}_i)$ is the action density at wave number $\boldsymbol{k}_i$, and G is a complicated coupling coefficient Herterich and Hasselmann, 1980), and δ is the Dirac delta function. We note that if the resonance relations in Eqs. (2) and ((3) are satisfied, then the delta functions in (5) takes on values of unity. On the other hand, the right hand side of (5) vanishes if the quadruplets do not satisfy (2) or (3).

The application of the full Boltzmann integral in operational models

is impractical since it is computationally costly (Tolman, 2013; van Vledder and Bottema, 2003). Several simpler and more computationally economical formulations, although with some disadvantage of loss of accuracy, have been proposed. The various formulations of the non-linear wave interactions are thus briefly discussed below.

(i) Discrete Interaction Approximation (DIA) – NL1

The discrete interaction approximation (DIA) source term was developed by Hasselmann et al. (1985) as a substitute for the full Boltzmann integral in order to make operational wave modelling computationally feasible. It is worth noting that the development of the DIA begun the journey for third generation ocean wave models for prediction (van Vledder and Bottema, 2003). In the DIA, only one wave number configuration and its mirror image are considered, and as shown in Eq. (2), the DIA assumes that $\boldsymbol{k}_1 = \boldsymbol{k}_2$, while $\boldsymbol{k}_3$ and $\boldsymbol{k}_4$ are considered to be of different magnitudes. The interaction is said to conserve energy, momentum and action. The DIA also replaced the complex coupling coefficient in Eq. (5) with a simple scaling function, which works only for deep water conditions. In order for the source term to function in shallow water, another scale function was introduced to resolve the effect of limited water depths (Hasselmann and Hasselmann, 1985). A detailed account of the DIA is presented by several authors (Polnikov, 2020; Tolman and Krasnopolsky, 2004; Tolman, 2004, 2013). The DIA has been used extensively in third generation wave models (Booij et al., 1999; Liu et al., 2019; Tolman, 1991; WAMDI Group, 1988). Despite its wide application, the DIA is noted to have several shortcomings. An example is the overestimation of interactions at frequencies that are above the spectral frequencies and thus produces broader spectra having higher energy levels (Tolman, 2013; Tolman and Chalikov, 1996), thus compromising the accuracy of wave parameters. The traditional DIA is also known to conserve all properties (energy, action and momentum) in deep water but fails to conserve momentum in shallow water. A detailed discussion of the shortcomings of the DIA is presented by Liu et al. (2019).

(ii) Generalized Multiple DIA – NL3

The generalized multiple DIA (GMD), developed by Tolman (2013), is an extension of the DIA. The essence of the GMD is to provide economical non-linear parameterisation term for operational wave modelling, while maintaining accuracy. Whereas the DIA was constructed mainly for deep water but with a scaling factor for shallow water, the GMD was constructed to accommodate arbitrary water depths (Liu et al., 2019; Tolman, 2013). The DIA considers only one set of quadruplets, whereas the GMD employs multiple representative quadruplets for interactions (Liu et al., 2019). The GMD also provides scaling functions for weak interactions in deep water as well as strong interactions in extreme shallow water conditions. Additionally, the GMD has many free parameters that can be optimized as opposed to only two for the traditional DIA with one quadruplet (Tolman and Grumbine, 2013). Each representative quadruplet in the GMD is described to have up to five free parameters.

The formulation of the GMD satisfied the resonance condition of representative quadruplets and introduced a reference frequency (σ_r) and an angular gap (θ_{12}) between the wavenumbers $\boldsymbol{k}_1$ and $\boldsymbol{k}_2$. According to Tolman (2013), satisfying the resonance condition assures the conservation of energy, action and momentum, which is a key property of nonlinear interactions. The use of σ_r and θ_{12} can be implicit to the quadruplet definition, or they can be explicitly tuneable parameters as applied in the WAVEWATCH III model. An advantage of the GMD over the traditional DIA is the conservation of momentum in shallow water since the representative quadruplets are evaluated for the actual water depth. Details on the progress and development of the GMD are presented in Tolman Hendrik (2010, 2013), Tolman and Grumbine (2013).

(iii) Exact interaction approximation – NL2

The exact interaction approximation method, also known as the Webb-Resio-Tracy (WRT) method for calculating the nonlinear interaction of waves is based on the original six-dimensional Boltzmann integral formulation of Hasselmann (1962, 1963a, 1963b), and other additions by Webb (1978), Tracy and Resio (1982) and Resio and Perrie (1991). The WRT method analytically transformed the Boltzmann integral by the elimination of the delta (δ) function indicated in Eq. (5). This function determines the location in a wavenumber space where integration should be carried out (van Vledder, 2002; van Vledder, 2012). The method was first initiated by Webb (1978) and was later incorporated by Tracy and Resio (1982) in a discrete deep-water spectra computational method. Later, a shallow water version of Webb's method was developed, which was implemented by Resio et al. (2001) to become the WRT method (van Vledder, 2006). The WRT method is currently applied in several third generation wave prediction models including WW3 (Tolman, 2002), SWAN (Booij et al., 2004), CREST (Ardhuin et al., 2001) and PROWAM (Monbaliu et al., 1999). It has the advantage of computing the non-linear transfer rate to any degree of accuracy (van Vledder, 2012).

(iv) Two-scale approximation – NL4

The two-scale approximation (TSA) source term for evaluating the full Boltzmann integral is based on previous formulations (Resio and Perrie, 1991; Tracy and Resio, 1982; Webb, 1978) referred to here as the WRT method. The source term assumes that the distribution of energy within a spectrum can be expressed as the sum of two primary scales (broad and local scales), and therefore decomposes a directional spectrum into a parametric (broad-scale) spectrum, a local-scale (non-parametric) component and a cross term (Perrie et al., 2013; Perrie and Resio, 2009; Resio and Perrie, 2008; van Vledder, 2006; WAVEWATCH III Development Group, 2016). The cross term represents the interaction between the broad and local-scale components of the wave spectrum (WAVEWATCH III Development Group, 2016). The broad-scale component is represented by a simple parametric form containing most of the energy in a wave spectrum, which in turn is based on few spectral variables consisting of peakedness, a Phillips-type equilibrium range coefficient and the directional distribution around the spectral peak direction (Perrie et al., 2013; WAVEWATCH III Development Group, 2016). In order to preserve the same degree of freedom as the original spectrum, the TSA represents the residual of the spectrum by a local perturbation-scale or second order term. This is indicated by Perrie et al. (2013) and Resio and Perrie (2008) as being essential to a detailed-balance source term formulation which involves S_{in}, S_{ds} and S_{nl} as seen in Eq. (1). The TSA has been reported to be more accurate than the DIA (Perrie et al., 2013; Perrie and Resio, 2009; Resio and Perrie, 2008).

2. Data and methods

2.1. Study location

The study involves the West Africa region which mainly includes the Canary Current and the Gulf of Guinea marine environments spanning between latitude 10° S to 30° N and longitude 35° W to 15° E. The wave model simulations were conducted for the entire study area as well as for two sub-regions of the study area designated as north-western sub-section (latitudes 10° N – 25° N; longitudes 30° W – 10° W), covering the Canary Current region, and south-eastern sub-section covering the Gulf of Guinea region (latitudes 2° S – 8° N; longitudes 10° W – 10° E). Fig. 1 shows the study area with the sub-divisions and *in-situ* measurement locations.

2.2. Data

2.2.1. Wind input data

Wind data for forcing the wave model was obtained from National Oceanic and Atmospheric Administration (NOAA) National Operational Model Archive and Distribution System (NOMADS). The wind data has a spatial resolution of 0.5 degrees latitude-longitude and a 6-hourly temporal resolution.

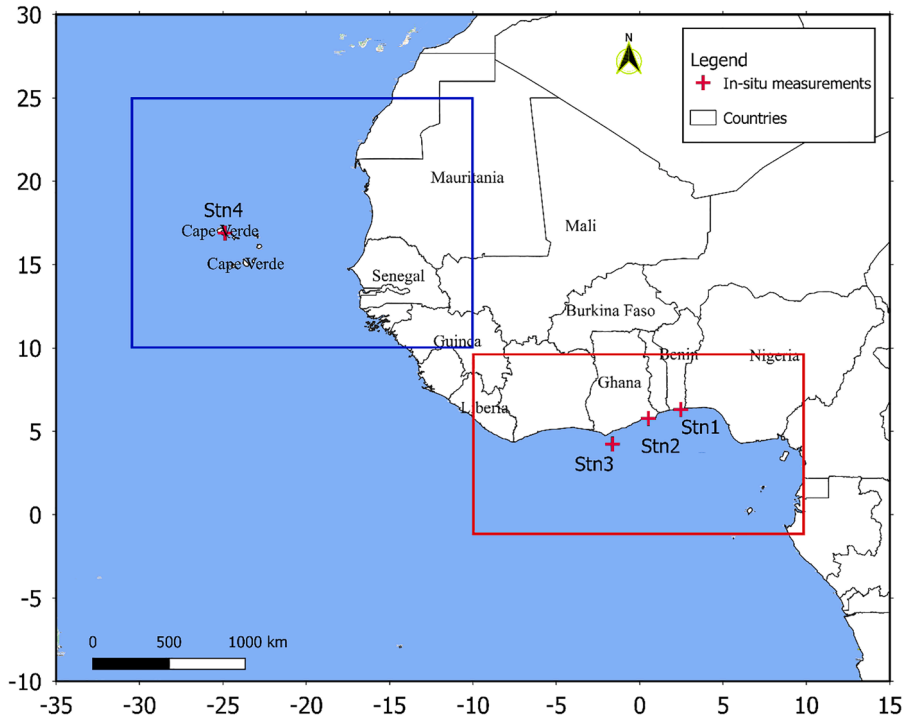

Fig. 1. Map of study area indicating stations of *in-situ* measuring equipment as red crosses, north-western sub-division as blue rectangle, and south-eastern sub-division as red rectangle for wave model simulations.

Table 1
Location of field wave measurements where *in-situ* data was obtained with collocated data period for model data comparison.

Station ID	Station Name / Location	Longitude	Latitude	Equipment Type	Data Source (Institution)	Estimated Depth of station (m)	Collocated Data Period / Model ran periods (yyyymmdd)
Station 1 (Stn1)	Cotonou, Benin	2.47	6.31	Alize Multi-parameter Oceanographic buoy	Institut de Recherches Halieutiques et Océanologiques du Bénin (IRHOB) (IRHOB), Benin	16.5	20151215 - 20160209
Station 2 (Stn1)	Ada, Ghana	0.52	5.77	Teledyne RD ADCP	International Marine and Dredging Consultants (IMDC), Antwerp, Belgium	11.5	20100219 - 20100316
Station 3 (Stn1)	Takoradi, Ghana	-1.63	4.23	Datawell Directional Wave buoy	Department of Marine and Fisheries Sciences, University of Ghana	170	20111012 - 20111121
Station 4 (Stn1)	Mindelo, Cabo Verde	-24.87	16.89	Triaxys Wave buoy	GMES and Africa programme, University of Ghana	70	20160204 - 20160412

2.2.2. Observational data

Independent *in-situ* datasets were obtained from three moored buoys and an Acoustic Doppler Current Profiler (ADCP) and comprised of significant wave height and wave direction information. Locations for the moored buoys are Cotonou in Benin (station 1 – Stn1), Takoradi in Ghana (station 3 – Stn3), and Mindelo in Cabo Verde (station 4 – Stn4). The ADCP was located at Ada in the eastern corridor of Ghana (station 2 – Stn2). Measurements from these instruments only covered short periods. Table 1 provides detailed information on the deployed *in-situ* measuring equipment and their locations.

2.3. Wave model setup

2.3.1. Generation of spatial grids

Version 5.16 of the WAVEWATCH III® model was used in the wave model simulations. The generation of model domain grid was by use of the GRIDGEN code (Chawla and Tolman, 2007) implemented in Matlab®. The domain grid comprised the entire area of West Africa with two sub-domains from the north-western and south-eastern sections of the main grid. The main grid has a spatial resolution of 0.25 degrees whiles the sub-grids have a resolution of 0.125 degrees. The extents of the domain grids are provided in Section 2.1 and shown in Fig. 1. Domain grids were generated from ETOPO2 bathymetry with regular rectilinear grids.

2.3.2. Wave model parameterization schemes

Four non-linear source terms (S_{nl}) implementable in WW3 were investigated in addition to application of no non-linear formulation (indicated as NL0), resulting in five formulations. These non-linear terms are the DIA (hereafter referred to as NL1), WRT (hereafter referred to as NL2), GMD (hereafter referred to as NL3) and TSA (hereafter referred to as NL4) methods. The input-dissipation source term by Tolman and Chalikov (1996) with wind correction factor (i.e. TC96stab or ST2STAB) was applied with all non-linear source terms. This is based on the outcome of previous studies by Foli et al. (2022) for the West Africa region. The parameterisation scheme for the model run comprised of a global time steps of 900 s and 450 s; spatial propagation time steps (CFL) of 950 s and 475 s; Maximum refraction (and wave-number shift) time steps of 450 s and 225 s; and Source term integration time steps of 15 s each for the main grid and the sub-grids respectively.

The main grid has 201×161 points with 58.9% comprising sea points. The north-western sub-grid on the other hand has 161×121

points with 67.2%, whereas the south-eastern sub-grid has 161×81 with 68.4% sea points. All grids were discretized with 32 frequencies from 0.0373 to 0.7159 Hz using a 1.1 increment factor and 36 directions with a 10° directional increment. Remaining details of the model setup is presented in WAVEWATCH III Development Group (2016).

2.4. Statistical comparisons

The outputs of the various simulations were compared statistically with *in-situ* measurements by estimating the mean bias ($\bar{\mu}$) and standard deviations (σ) and correlation coefficients (r). The mean bias is the mean of the difference between the model simulations and measured data. A normalized bias index (*NBI*) as well as the symmetrically normalized root mean square error (HH) index proposed by Hanna and Heinold (1985) were also computed. The HH index is an accuracy performance index that can be used in differentiating the performance of numerical models (Mentaschi et al., 2013). Relatively lower HH index values indicate the best models. Similarly, NBI values closer to zero depict best fit between model and observed data.

3. Results and discussions

This study presents results from investigating appropriate non-linear wave-wave interaction source terms (S_{nl}) to be used in the West Africa region for projecting ocean waves. Four different S_{nl} were investigated, with an additional simulation implemented with no non-linear term (NL0). The results are compared with *in-situ* observed data taken from four different geographical locations in the region (Fig. 1). The S_{nl} are represented as NL0, NL1, NL2, NL3 and NL4 as defined in previous sections. Results for the entire West Africa grid as well as for two subdivisions (south-eastern – SE, and north-western – NW sub-sections) are presented. Results for NL4 have been eliminated from the plots and analysis because of spurious behaviour with large errors at most of the stations. This spurious effect has also been documented by Auclair (2011) when a third order propagation scheme is employed, as implemented in this study. This was attributed to have originated from the high frequency component of the spectrum (Auclair, 2011).

3.1. West Africa grid

Simulations for the entire West Africa grid show that at station 1 (Stn1), projected significant wave heights (H_s) did not agree very well with measured data (Figs. 2 and 3). Large deviations occur between measured data and the simulations. A similar situation is true for station 3, but with better performance. This is shown by a scatterplot of measured data against simulations (Fig. 4). Simulations for stations 2 and 4 however were in close agreement with measured data. The patterns of (dis)agreement at the various stations is similar to observations by Foli et al. (2022) which has been attributed to errors in the input winds. Wave directions on the other hand have close agreements with measured data for all stations as compared to wave height simulations (Fig. 5, 6 and 7).

The performance of simulations for S_{nl} at station 1 (Stn1) indicates that NL0 best estimates wave heights with least HH index of 0.833 and NBI of -52.71% (Table 2). This is followed closely by NL1 with HH index and NBI of 1 and -60.47% respectively. This is clearly illustrated in Fig. 8, which provides a plot of HH against NBI as a measure of model performance. Although NL0 recorded the least HH, NBI as well as mean bias values for significant wave heights, it also recorded the highest bias standard deviation (0.27 m). Similarly, NL2 best estimates wave directions for Stn1 with mean bias, HH and NBI of 6.76±29.97 °, 0.15 and 3.55% respectively. This is again followed closely by NL3. Station 1 exhibits weak correlations for both wave heights and directions (Tables 2 and 3).

At station 2, wave heights recorded low bias standard deviations for all source terms (Fig. 3 and Table 2). However, NL0 produced the least mean bias (-0.04 ± 0.16 m), HH index (0.189) and NBI (4.65%), followed by NL2 (Table 2 and Fig. 8). Although NL2 recorded the highest correlations (0.87) among the source terms, it would be considered secondary after NL0, which has the least HH and NBI as the preferred measure of performance. Wave directions are also best estimated by NL3 with Mean bias, HH and NBI of 2.23 ± 11.77 °, 0.061 and 1.17% respectively. NL1 followed NL3 closely in estimating wave directions at Stn2 with HH and NBI of 0.062 and 1.27% respectively (Table 3 and Fig. 8).

At station 3, although high deviations were recorded for wave heights, some source terms still produced appreciable trends (Fig. 2). Here, wave heights are best estimated by NL1 with HH index and NBI of

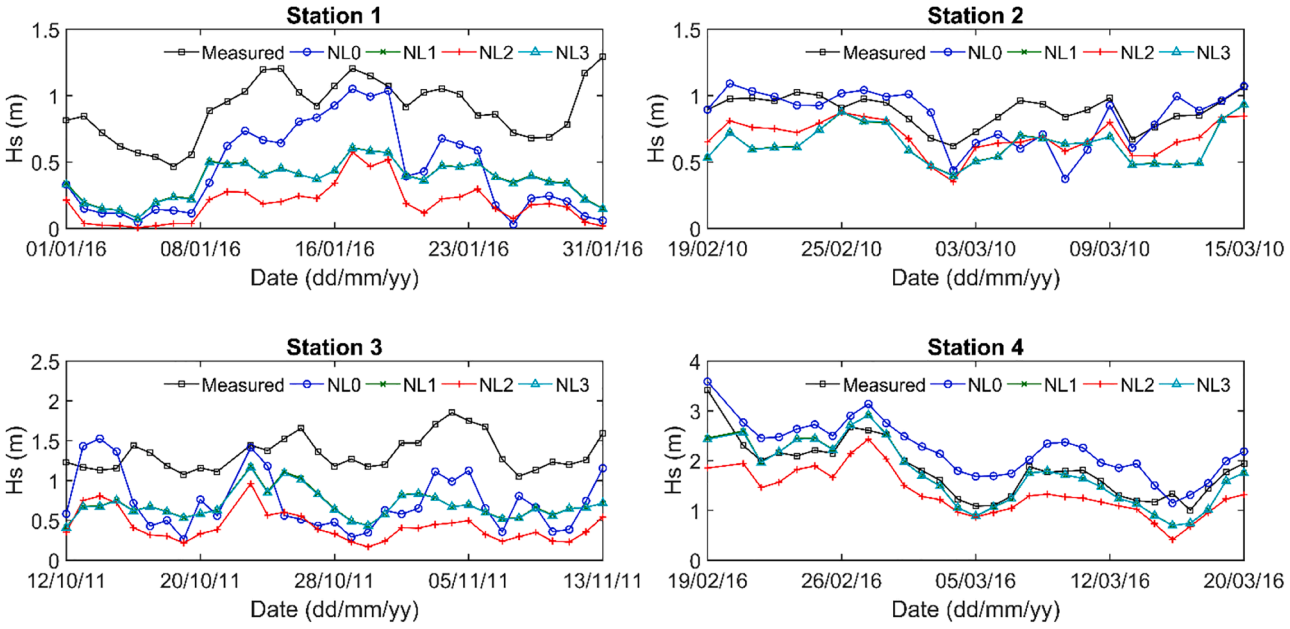

Fig. 2. Time series plot of significant wave height (H_s) outputs for the West Africa grid.

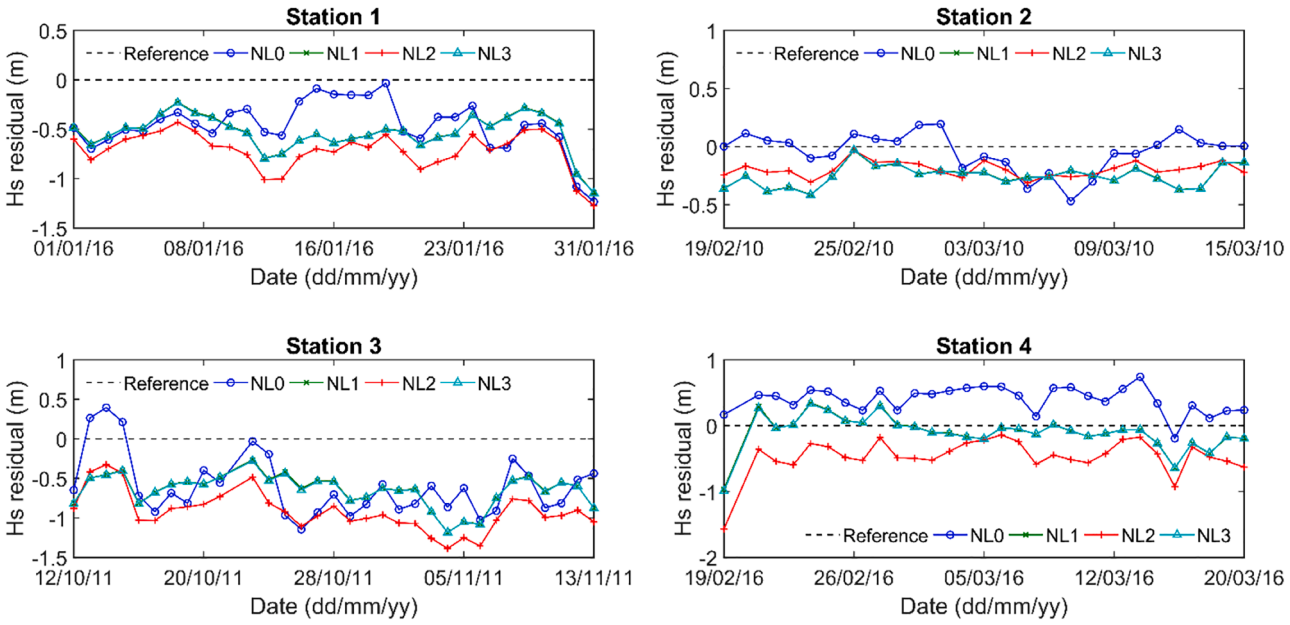

Fig. 3. Time series plot of wave height residuals/bias for the West Africa grid.

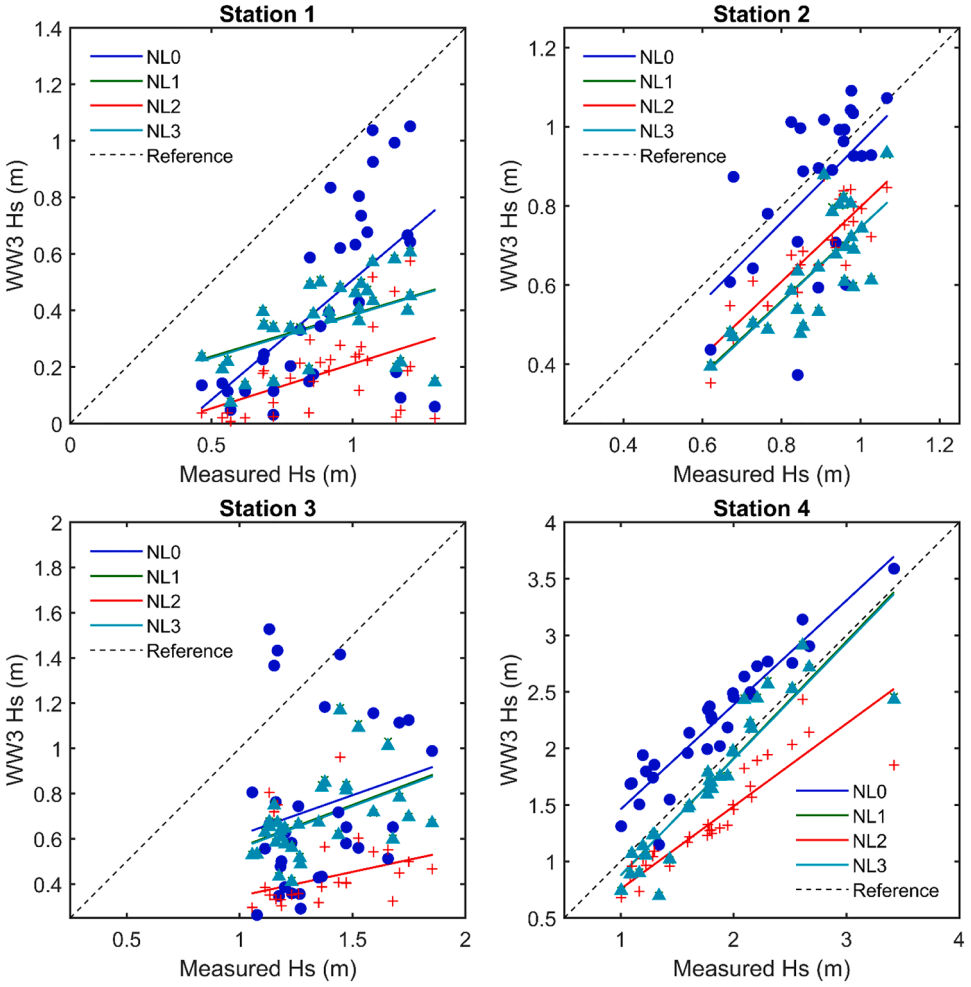

Fig. 4. Scatter plot of measured significant wave heights (H_s) against model significant wave heights for the West Africa grid. Black dotted lines are references while solid lines are the linearly fitted lines for the various model source terms.

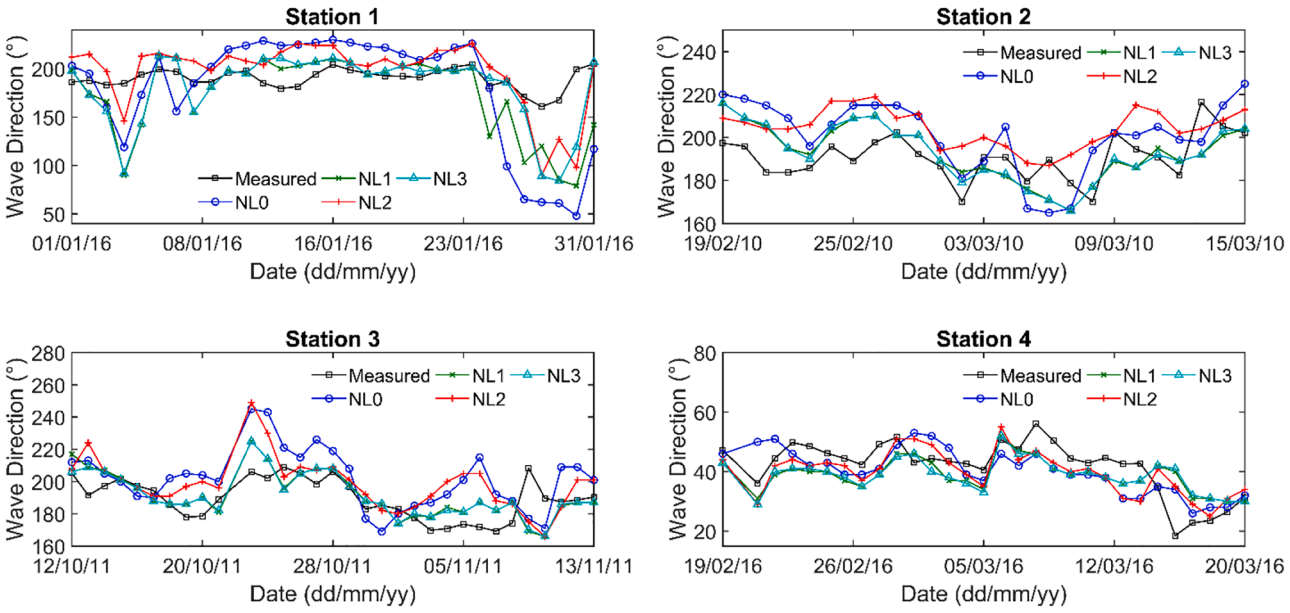

Fig. 5. Time series plot of wave direction outputs for the West Africa grid.

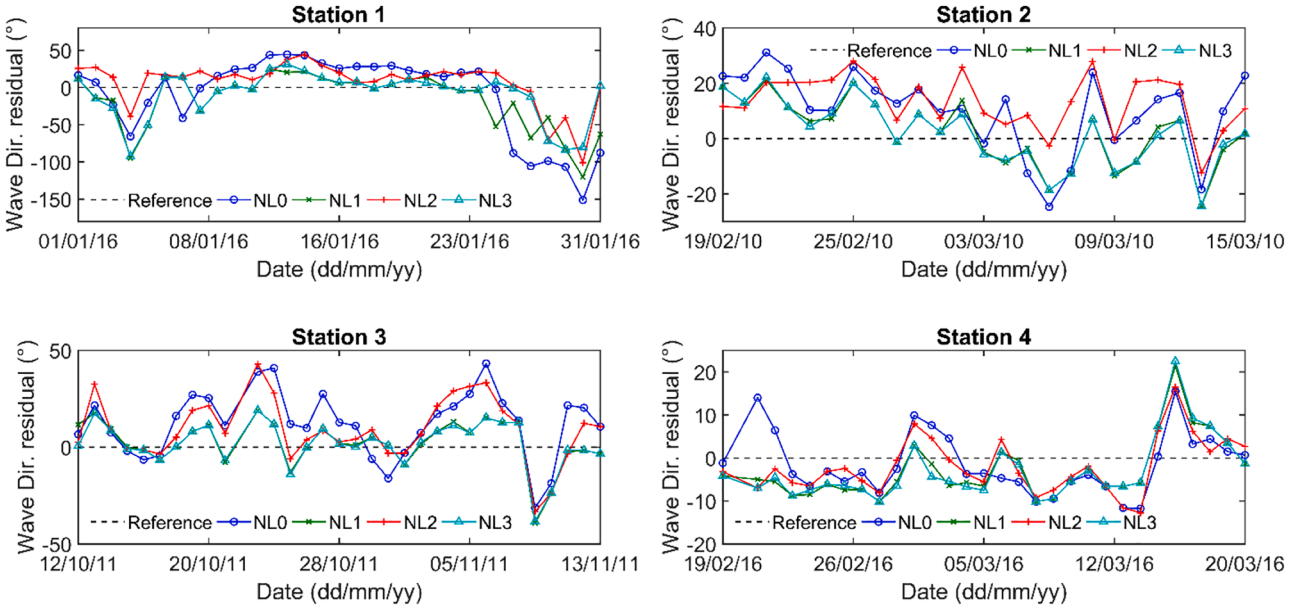

Fig. 6. Time series plot of wave direction residuals/bias for the West Africa grid.

0.703 and -48.55% respectively (Table 2 and Fig. 8). NL0 and NL3 with the same HH indices of 0.71 follows NL1. However, NL0 produces a lower NBI compared to NL3 and therefore would be considered to better estimate wave heights after NL1. Wave directions on the other hand are best estimated by NL3 and followed very closely by NL1 (Table 3). NL1 and NL3 have the same HH values (0.06) and correlation coefficients (0.59). However, NL3 produces lower mean bias (1.81±11.81 °) and NBI (0.95%) compared to NL1 (2.22±12.1 ° and 1.17% respectively), thus making NL3 the best estimator of wave directions at this station and followed by NL1.

Simulations recorded very good agreements with *in-situ* measurements at Stn4 for both wave heights and directions (Figs. 2, 3, 5 and 6). Interestingly, NL1 and NL3 again recorded same values of mean bias (-0.1±0.26 m), correlation coefficient (0.91) and HH (0.15) for wave height estimations (Table 2). NL1 however produced a better percentage error (NBI of -5.35%) compare to NL3 (NBI of -5.54%). Thus, NL1 is the best estimator of wave height for Stn4, with NL3 being next. For wave direction estimations, all source terms produced correlation coefficient of 1 (Table 3), indicating very good performance of all source terms in projecting wave directions at station 4. Nonetheless, NL2 outperforms all the source terms with slight margins in the performance indices, followed by NL0. The high level of performance of the source terms at St4 has been indicated by Foli et al. (2022) to be partially attributable to the accuracy in wind input among other factors. The performance and accuracy of different wind input sources from the investigations of Foli et al. (2021) revealed that St4 records higher accuracies in modelled wind fields from the National Centers for Environmental Prediction (NCEP) and the European Centre for Medium-Range Weather Forecasts (ECMWF) compared to other locations in the region. This they (Foli et al., 2021) suggested could be as a result of increased *in-situ* data collection and assimilation for this particular location (St4).

A combination of all stations as a representation for the entire West

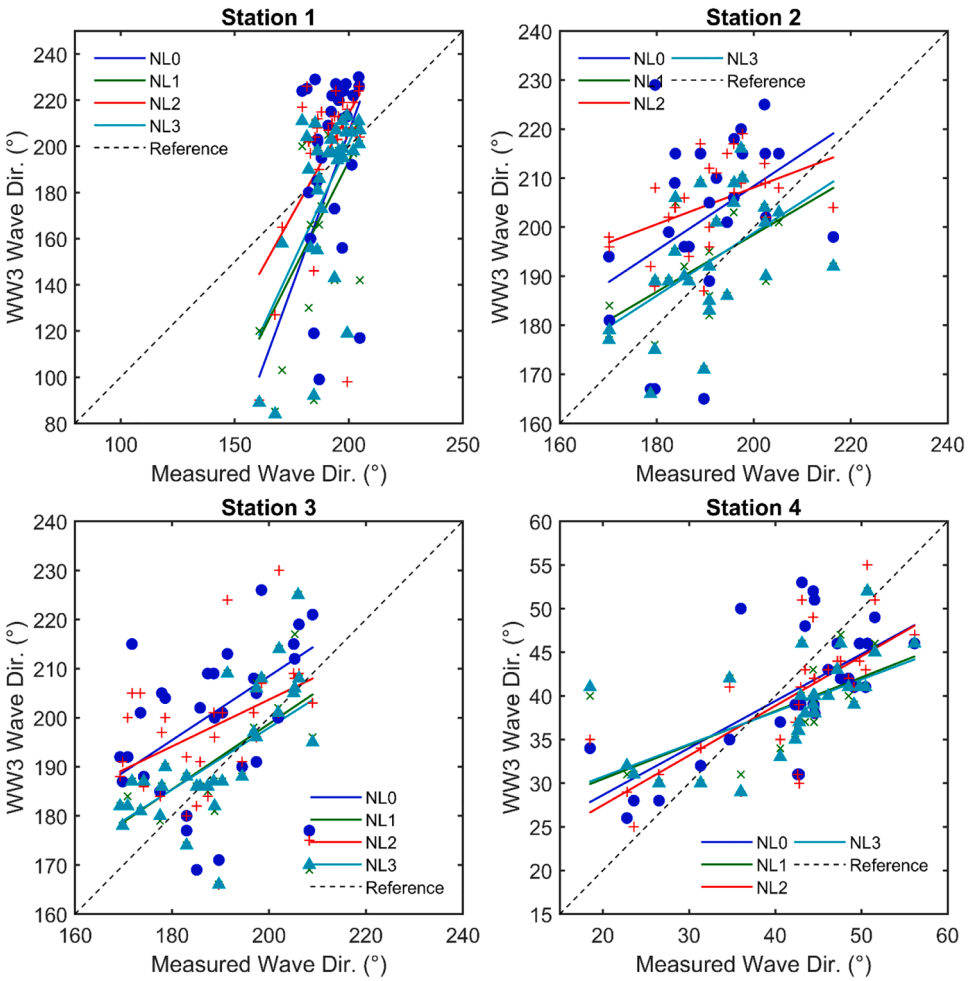

Fig. 7. Scatter plot of measured against model wave directions for the West Africa grid. Black dotted lines are references while solid lines are the linearly fitted lines for the various model source terms.

Table 2
Summary of wave height statistics for comparisons of model simulations with *in-situ* measurements for entire West Africa grid (S_{nl}).

Location	Source Term (Snl)	Mean bias (m)	Bias Standard Deviation	Correlation coefficient (R)	HH-Index	NBI
Station 1	NL0	-0.48	0.27	0.58*	0.833	-52.71
	NL1	-0.55	0.2	0.47*	1	-60.47
	NL2	-0.73	0.2	0.48*	1.773	-80
	NL3	-0.55	0.2	0.48*	1.011	-60.9
Station 2	NL0	-0.04	0.16	0.58*	0.189	-4.65
	NL1	-0.25	0.09	0.76*	0.345	-27.8
	NL2	-0.2	0.06	0.87*	0.26	-22.1
	NL3	-0.25	0.09	0.76*	0.347	-27.98
Station 3	NL0	-0.6	0.39	0.21	0.71	-45.04
	NL1	-0.65	0.21	0.47*	0.703	-48.55
	NL2	-0.92	0.25	0.25	1.26	-68.7
	NL3	-0.66	0.21	0.47*	0.71	-48.92
Station 4	NL0	0.4	0.19	0.94*	0.214	22.08
	NL1	-0.1	0.26	0.91*	0.15	-5.35
	NL2	-0.46	0.27	0.88*	0.327	-25.52
	NL3	-0.1	0.26	0.91*	0.15	-5.54
All Stations	NL0	-0.2	0.48	0.81*	0.41	-15.89
	NL1	-0.4	0.3	0.88*	0.43	-31.96
	NL2	-0.6	0.34	0.77*	0.69	-48
	NL3	-0.4	0.3	0.88+	0.44	-32.25

* indicate significant correlations, i.e. $p < 0.05$

Africa region indicates NL0 as the best estimator of significant wave heights, with mean bias, HH and NBI of -0.2±0.48 m, 0.41 and -15.89% respectively. NL1 and NL3 equally follow NL0 in estimating wave heights with the same mean bias (-0.4±0.3 m), HH (0.43) and correlation coefficient (0.88). NL1 however slightly outperforms NL3 with a lower percentage error (NBI) of -31.96% and therefore would be considered the next best estimator of wave heights after NL0 for the entire West Africa region. Apart from Stn1 for wave directions, NL1 and

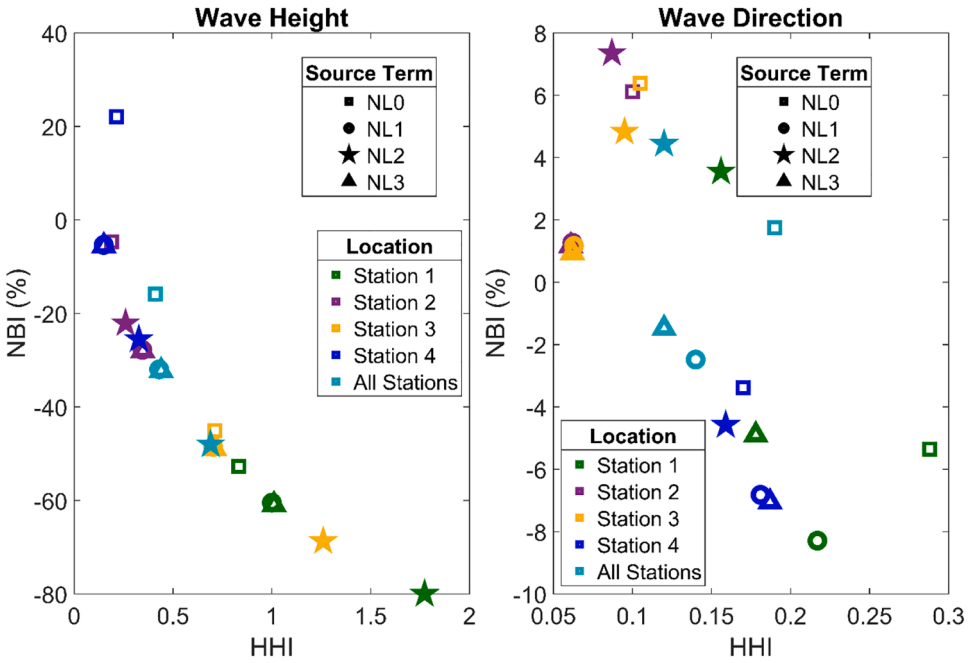

Fig. 8. Plots of HH against NBI for significant wave heights (left) and wave directions (right) for all stations of the West Africa grid.

Table 3
Summary of wave direction statistics for comparisons of model simulations with *in-situ* measurements for entire West Africa grid (S_{nl}).

Location	Source Term (Snl)	Mean bias (°)	Bias Standard Deviation (°)	Correlation coefficient (R)	HH-Index	NBI
Station 1	NL0	-10.18	53.39	0.5*	0.288	-5.35
	NL1	-15.77	37.04	0.51*	0.217	-8.29
	NL2	6.76	29.97	0.55*	0.156	3.55
	NL3	-9.33	32.27	0.6*	0.178	-4.9
Station 2	NL0	11.65	16.16	0.41*	0.1	6.11
	NL1	2.42	11.91	0.49*	0.062	1.27
	NL2	14	10.34	0.46*	0.087	7.35
	NL3	2.23	11.77	0.53*	0.061	1.17
Station 3	NL0	12.09	17.01	0.44*	0.105	6.38
	NL1	2.22	12.1	0.59*	0.06	1.17
	NL2	9.15	16.2	0.37*	0.095	4.83
	NL3	1.81	11.81	0.59*	0.06	0.95
Station 4	NL0	-1.41	7.05	1*	0.17	-3.38
	NL1	-2.85	6.93	1*	0.181	-6.82
	NL2	-1.91	6.4	1*	0.159	-4.58
	NL3	-2.95	7.11	1*	0.187	-7.05
All Stations	NL0	2.68	31.22	0.91*	0.19	1.75
	NL1	-3.8	22.23	0.95*	0.14	-2.48
	NL2	6.8	19.15	0.97*	0.12	4.44
	NL3	-2.26	19.27	0.96*	0.12	-1.48

* indicate significant correlations, i.e. $p < 0.05$

NL3 at all other stations very closely estimate both wave heights and directions, producing close performance indices, and thus resulting in difficulty in distinguishing between these two source terms in the figures. The results tables (Tables 2 and 3) however provide the distinction between the two.

Apart from simulations for NL0 at station 4, all source terms underestimated the wave heights at all the stations (Table 2). Wave directions on the other hand are best estimated by NL3, followed closely by NL2 (Table 3 and Fig. 8) for the combined stations. While wave directions are overestimated by NL2 by 4.44%, they are underestimated by NL3 by just -1.48%.

As indicated by Foli et al. (2022), the WAVEWATCH-III model estimates wave directions better than wave heights in the West Africa region. The same result has been found in this study even though a different set of source terms have been employed.

3.2. Sub-grids of West Africa

Wave heights and directions obtained from simulations for the south-eastern grid are similar to those for the entire West Africa grid. Very little or no differences can be observed between the simulations on the low resolution West Africa grid and the high resolution south-eastern grid (Figs. 9–12).

Similar to simulations for the West Africa grid, wave height projections for Stn1 for the south-eastern grid also showed high levels of deviations despite the higher resolution grid used. This may be due to errors introduced during wind interpolation, or the model may perform better on a relatively coarse resolution grid compared to finer resolutions as reported by Foli et al. (2022). For this simulation, NL1 outperformed all source terms with mean bias and HH index of -0.65±0.23 m and 1.374 respectively (Table 4). Again, this is followed closely by NL3 with mean bias and HH index of -0.65±0.22 m and 1.403

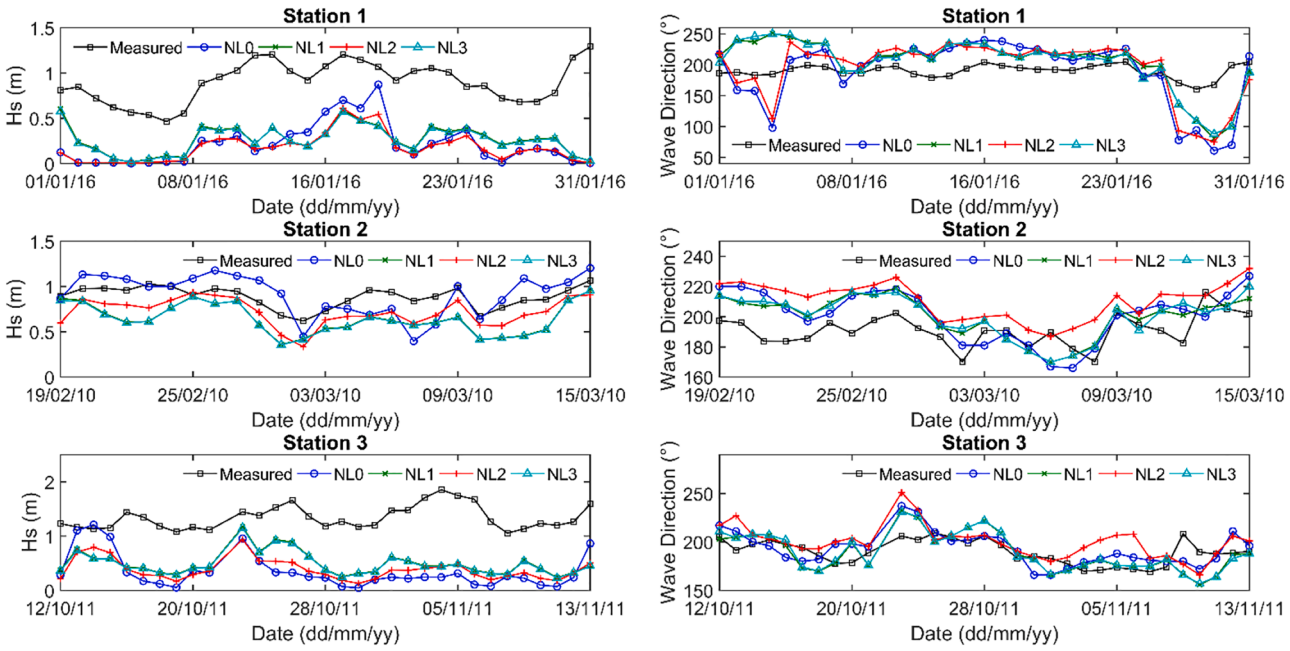

Fig. 9. Time series plot of significant wave height (left) and wave direction (right) outputs for the south-eastern grid.

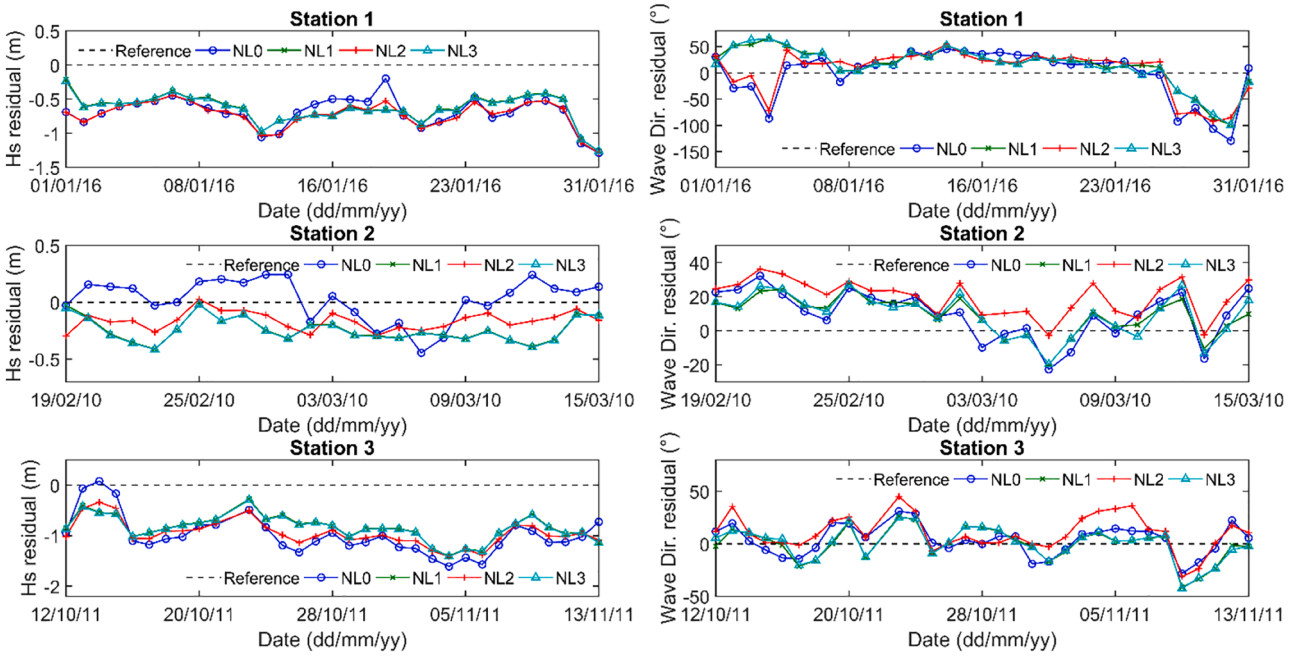

Fig. 10. Time series plot of residuals/bias of significant wave height (left) and wave direction (right) outputs for the south-eastern grid.

respectively. For wave directions at Stn1, NL3 alternately outperforms all the other source terms, followed by NL1 (Table 5). Low but significant correlation coefficients were observed for wave directions from Stn1 for all source terms.

At Stn2, NL0 had the best performance for wave heights with very low mean bias, HH index and NBI of +0.03±0.18 m, 0.197 and 2.86% respectively. This is the best performance among all source terms for the entire south-eastern sub-region for wave height estimations. NL2 follows with a mean bias, HH index and NBI of -0.16±0.08 m, 0.223 and -18.41% respectively. Wave directions on the other hand are best estimated by NL1 followed by NL3.

High deviations in wave heights also resulted in low correlation coefficients for all source terms at Stn3. NL1 and NL3 however well estimate wave height at Stn3. A mean bias of -0.85±0.25 m, with HH and NBI values of 1.078 and -63.31% makes NL1 a better predictor of wave heights over NL3 with mean bias, HH and NBI values of -0.86 m, 1.097 and -63.94% respectively. Wave directions at Stn3 are best estimated with NL0, which recorded the least HH index of 0.076 (Table 5). NL3 estimates wave directions with the least percentage error of 0.08% and follows NL0 as the next option for Stn3.

A combination of all the stations in the south-eastern sub-region for the sub-grid simulations reveals NL1 as the best estimator of significant wave heights, followed by NL3. Both NL1 and NL3 recorded the same mean bias and correlation coefficient of -0.6±0.32 m and 0.26 respectively (Table 4). However, while NL1 recorded HH and NBI values of 0.97 and -56.88%, NL3 recorded 0.98 and -57.53% respectively. Wave

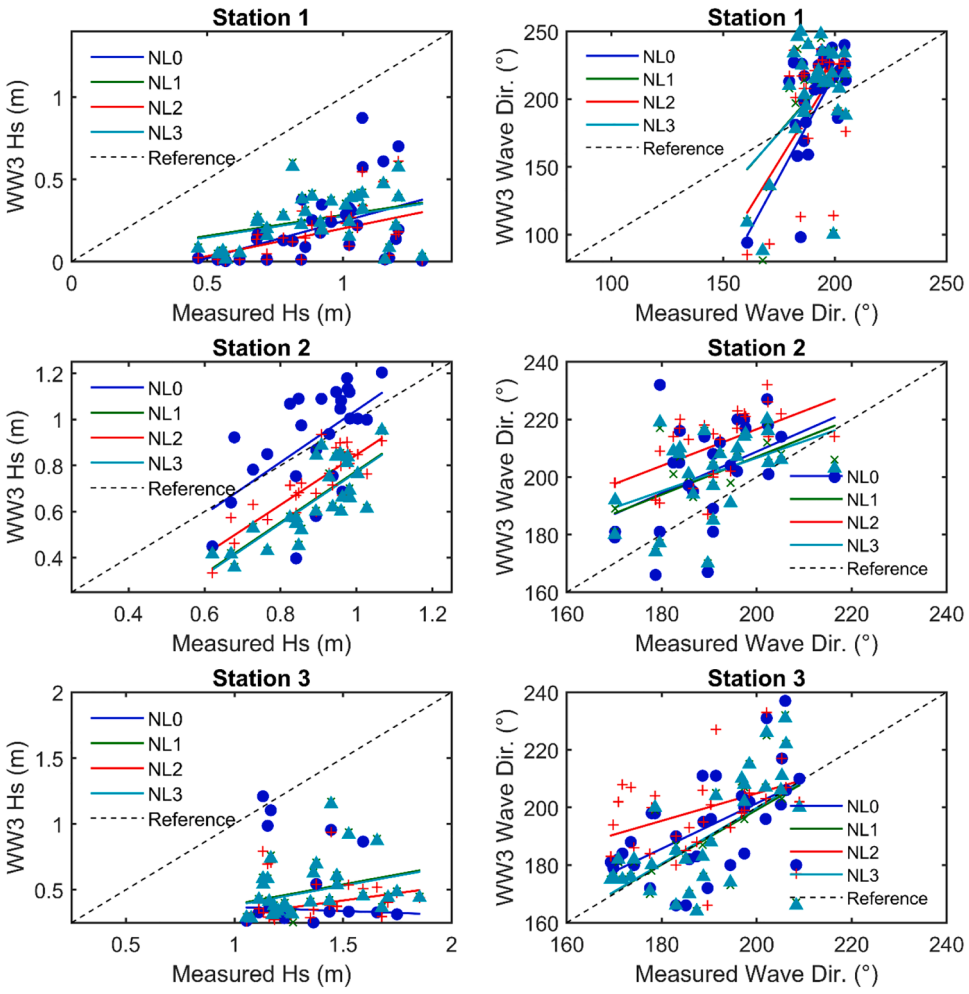

Fig. 11. Scatter plot of measured against modelled significant wave heights (left) and wave directions (right) for the south-eastern grid. Black dotted lines are references while solid lines are the linearly fitted lines for the various model source terms.

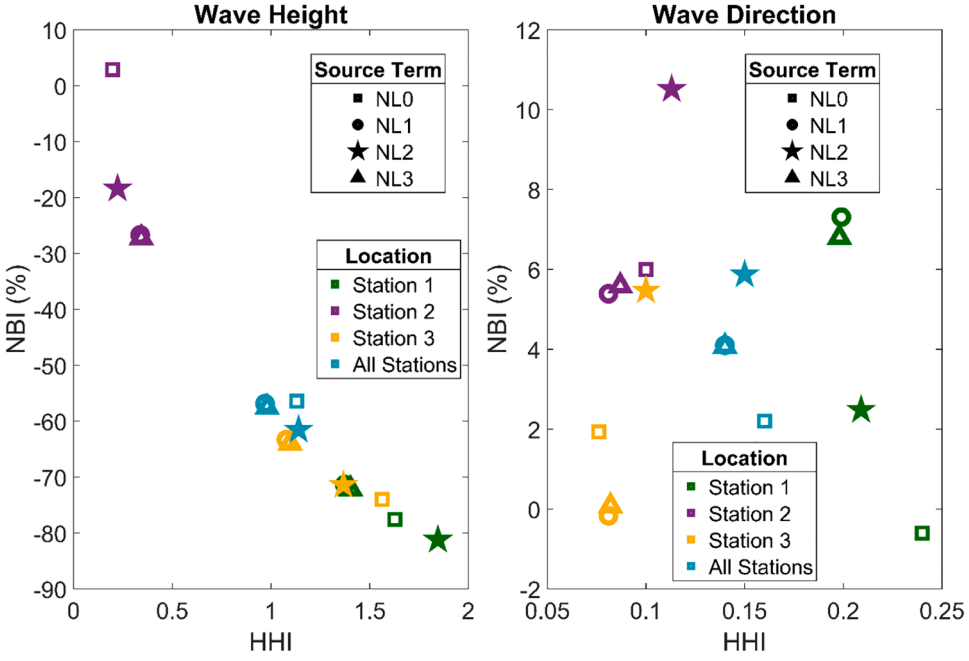

Fig. 12. Plots of HH against NBI for significant wave heights (left) and wave directions (right) for all stations of the south-eastern grid.

Table 4
Summary of wave height statistics for comparisons of model simulations with *in-situ* measurements for south-eastern and north-western sub-grids of West Africa grid (S_{nl}).

Model Grid	Location	Source Term (S_{nl})	Mean bias (m)	Bias Standard Deviation (m)	Correlation coefficient (R)	HH-Index	NBI
South-east	Station 1	NL0	-0.7	0.23	0.46*	1.627	-77.56
		NL1	-0.65	0.23	0.36	1.374	-71.36
		NL2	-0.74	0.2	0.48*	1.846	-81.22
		NL3	-0.65	0.22	0.37*	1.403	-72.13
	Station 2	NL0	0.03	0.18	0.59*	0.197	2.86
		NL1	-0.24	0.11	0.77*	0.337	-26.69
		NL2	-0.16	0.08	0.85*	0.223	-18.41
		NL3	-0.24	0.11	0.78*	0.343	-27.22
	Station 3	NL0	-0.99	0.39	-0.04	1.563	-74.02
		NL1	-0.85	0.25	0.31	1.078	-63.31
		NL2	-0.96	0.25	0.25	1.367	-71.44
		NL3	-0.86	0.25	0.31	1.097	-63.94
	All South-east Stations	NL0	-0.6	0.51	-0.08	1.13	-56.43
		NL1	-0.6	0.32	0.26*	0.97	-56.88
		NL2	-0.65	0.38	0.1	1.14	-61.55
		NL3	-0.61	0.32	0.26*	0.98	-57.53
North-west	Station 4	NL0	1.63	0.99	0.7*	0.733	90.23
		NL1	-0.27	0.26	0.91*	0.21	-14.78
		NL2	-0.51	0.3	0.85*	0.37	-28.38
		NL3	-0.27	0.26	0.91*	0.21	-15.01

* indicate significant correlations, i.e. $p < 0.05$

Table 5
Summary of wave direction statistics for comparisons of model simulations with *in-situ* measurements for south-eastern and north-western sub-grids of West Africa grid (S_{nl}).

Model Grid	Location	Source Term (S_{nl})	Mean bias (^{o})	Bias Standard Deviation (^{o})	Correlation coefficient (R)	HH-Index	NBI
South-east	Station 1	NL0	-1.15	46.46	0.62*	0.24	-0.6
		NL1	13.92	37.41	0.49*	0.199	7.31
		NL2	4.73	40.88	0.61*	0.209	2.48
		NL3	12.95	37.4	0.48*	0.198	6.8
	Station 2	NL0	11.42	16.28	0.44*	0.1	5.99
		NL1	10.27	12.45	0.51*	0.081	5.39
		NL2	20.03	10.64	0.57*	0.113	10.51
		NL3	10.65	13.68	0.43*	0.087	5.59
	Station 3	NL0	3.65	14.34	0.57*	0.076	1.93
		NL1	-0.32	15.59	0.61*	0.08	-0.17
		NL2	10.37	16.78	0.36*	0.1	5.47
		NL3	0.15	15.74	0.61*	0.08	0.08
	All South-east Stations	NL0	4.19	30.39	0.49*	0.16	2.2
		NL1	7.8	25.59	0.47*	0.14	4.1
		NL2	11.16	27.39	0.45*	0.15	5.87
		NL3	7.73	25.67	0.46*	0.14	4.07
North-west	Station 4	NL0	-1.88	5.84	1*	0.146	-4.5
		NL1	1.49	7.56	1*	0.176	3.56
		NL2	-0.48	6.56	1*	0.153	-1.15
		NL3	1.45	7.49	1*	0.175	3.48

* indicate significant correlations, i.e. $p < 0.05$

directions for the combined stations of the south-eastern grid are also best estimated by NL3 and supported by NL1 alternately. Fig. 12 depicts how closely matched the results for NL1 and NL3 are with each other. Although NL1 and NL3 recorded the same HH index (0.14) for the wave directions, NL3 recorded insignificantly lower NBI (4.07%) and mean bias (7.73±25.67 ^{o}), making NL3 the fore estimator of wave directions. NL1 and NL3 can therefore be interchanged without any significant loss in wave direction accuracy as can be seen in Fig. 12. This means that NL1, which is the best estimator of significant wave heights can equally well estimate wave directions for the south-eastern sub-region of the study area.

Simulations for the north-western sub-section, represented only by station 4 show that NL0 does not perform very well in estimating significant wave heights although it does relatively well in estimating wave directions (Fig. 13). NL0 produced very high HH index and percentage error (Table 4). Similar to the combined stations of the south-eastern grid, the significant wave heights in the north-western section are best estimated by NL1 and again followed closely by NL3. Again, NL1 and NL3 recorded the same mean bias (-0.27±0.26 m), correlation coefficient (0.91) and HH index (0.21) (Fig. 14). NL1 however recorded the least NBI (-14.78%) compared to that of NL3 (-15.01%), thus making it the fore estimator of wave heights for the north-western section. For wave directions, all source terms recorded correlation coefficient of 1. NL0 and NL2 recorded relatively low HH indices. Although NL2 recorded the least mean bias, it recorded a higher mean bias standard deviation. NL2 also recorded the least percentage error (NBI = -1.15%) among the source terms for the simulations in this sub-region. Despite this performance by NL2, NL0 best estimates wave directions with the least HH index of 0.146. It should however be noted that for wave direction estimations, differences in performance by the source terms are relatively low and therefore interchanging the source terms would not adversely affect the accuracy of the wave direction outputs as indicated by the results. Since NL1 has been shown to best estimate significant wave heights, it can also be used in estimating the wave directions for the north-western sub-region with respect to the high resolution north-western sub-grid.

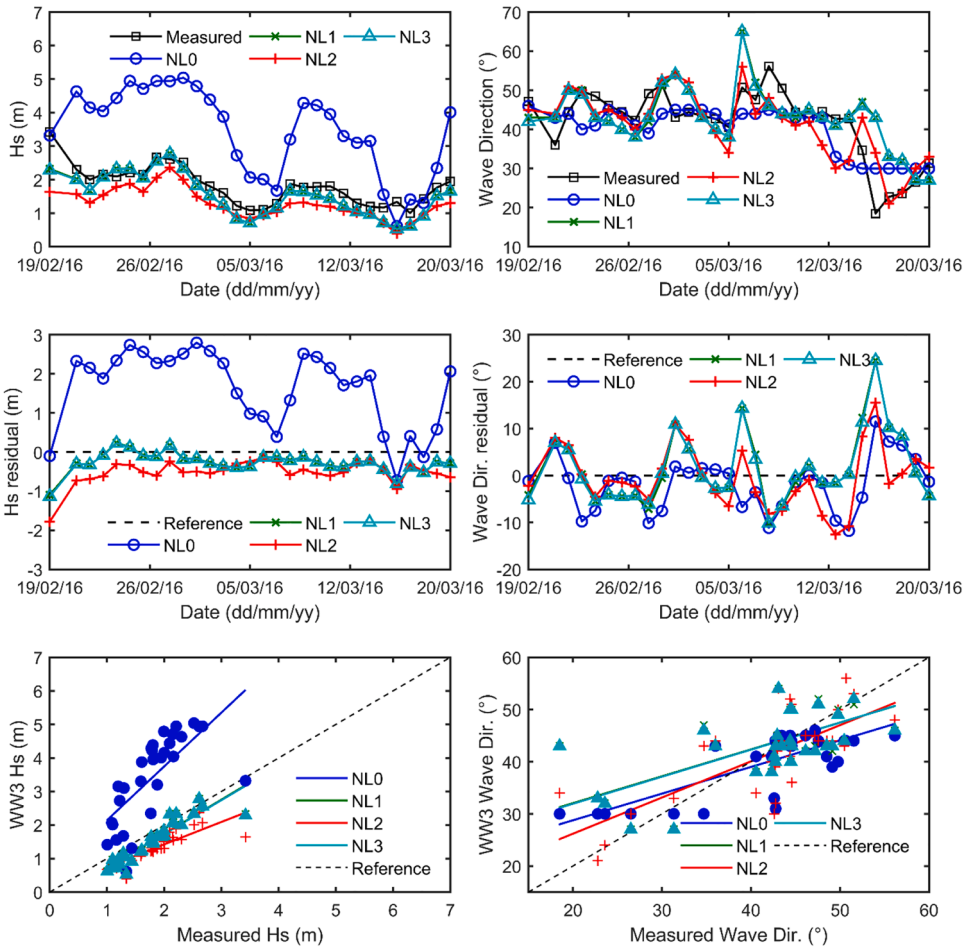

Fig. 13. Plots of significant wave heights (left) and wave directions (right) for the north-western grid. Top: Time-series of significant wave heights and directions; Middle: Time-series of residuals of significant wave heights and directions; Bottom: Scatter plots of measured against modelled significant wave heights and directions.

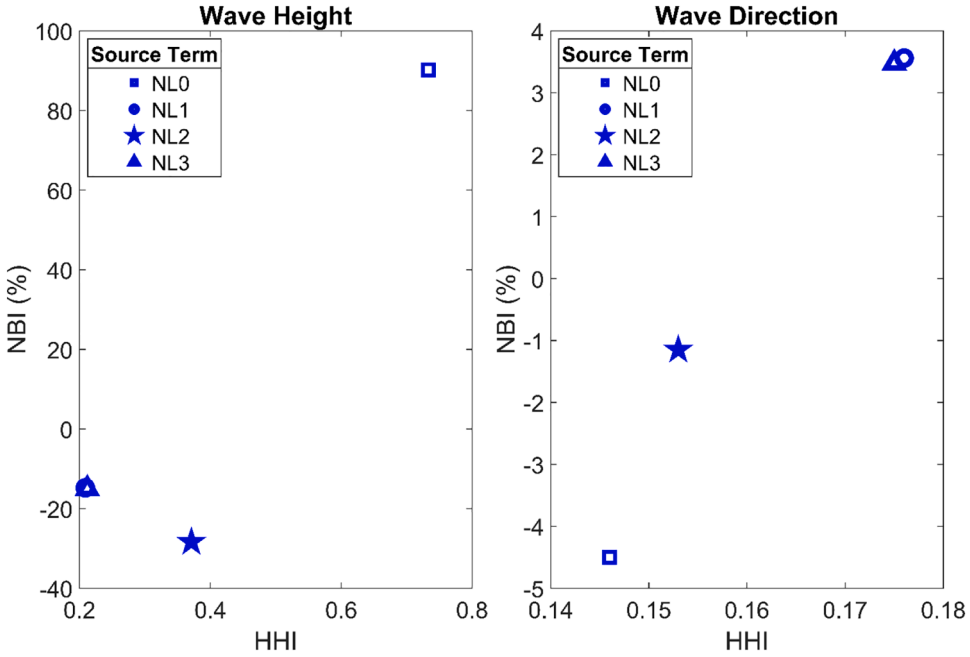

Fig. 14. Plots of HH against NBI for significant wave heights (left) and wave directions (right) for the north-western grid.

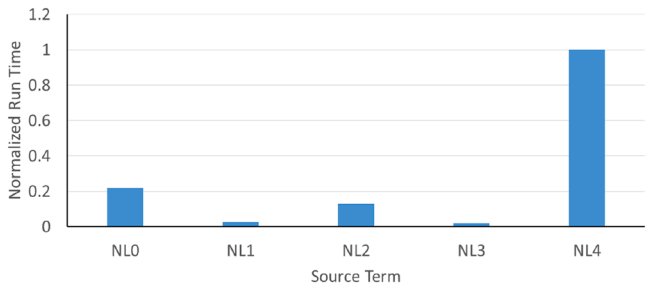

Fig. 15. Summary of overall model run-time performance of non-linear source terms investigated. Run time is normalized by the maximum time of 1,428,345.286 s (397 h).

As recorded by Foli et al. (2022), both wave heights and directions from simulations on the low resolution West Africa grid perform better than on the high resolution south-eastern and north-western sub-grids. The low resolution West Africa grid recorded lower HH indices and percentage errors (NBI) compared to the high resolution south-eastern and north-western sub-grids. This phenomenon has been attributed to the degree to which the wind is interpolated, which results in loss of accuracy beyond an optimum limit (Holt and Cavaleri, 1994; Mentaschi et al., 2015).

Model runtime for the non-linear source terms varied widely. Fig15 shows the range of model runtime observed during the simulations. NL4 recorded the longest runtime in addition to producing spurious effect. This is followed by NL0, which had a relatively normalized runtime of about 22%. The NL2 emerged as the third slow source term. The fastest executing source term is however NL3, with a relative normalized runtime of about 1.9%. This is seconded by NL1 with a relative normalized runtime of about 2.7%. NL1 and NL3 source terms are therefore best suited for projecting wave heights and directions not only with respect to the level of accuracy, but also with respect to the time spent in generating model outputs.

The Environmental Modelling Center of National Centers for Environmental Prediction (NCEP) under the National Oceanic and Atmospheric Administration (NOAA) reports of using NL1 non-linear source term in combination with Ardhuin et al. (2010) input-dissipation source term (ST4) in producing their wave forecast products on a multigrid for their global products (NOAA National Centers for Environmental Prediction, 2020). This study at the regional level for the entire West Africa grid, has found NL0 most suitable for this purpose, while identifying NL1 and NL3 most appropriate for the sub-sections of the study area.

4. Summary and conclusions

This study investigated the performance of selected non-linear wave-wave interaction source terms in the West Africa region in projecting ocean wave properties such as significant wave heights and directions. Five non-linear configurations were used in simulating the wave model. These are 1) formulations without any non-linear term – NL0; 2) Discrete Interaction Approximation (DIA) – NL1; 3) Exact Interaction Approximation – NL2; 4) Generalized Multiple DIA – NL3; and 5) Two-Scale Approximation – NL4.

Simulations of the non-linear source terms were conducted for the entire West Africa region level as well as for two sub-divisions (south-eastern and north-western sections) of the study area. NL4 was found to produce spurious outputs on all grids, resulting in very high level of errors in the outputs. Thus, the results for NL4 were removed from the analysis. Different source terms provide best estimates of wave heights and directions for the various stations where *in-situ* data was obtained and compared with model outputs. For the entire West Africa grid, NL0 best estimates significant wave heights whereas NL3 best estimates wave directions. Similarly, while NL1 best estimates wave heights for the combined south-eastern grid, NL3 best estimates the wave directions although this can be alternated with NL1 because of insignificant differences between the two source terms in estimating wave directions.

For the north-western sub-region of the study area, NL1 best estimates significant wave heights while NL0 best estimates wave directions, with similar ability to alternate with NL2 in projecting wave directions. The results have shown that insignificant differences exist between the source terms in projecting wave directions, especially for the north-western section. This means that any of the non-linear source terms may be used in projecting wave directions without significantly compromising on accuracy. This implies that NL1, which best estimates significant wave heights for the north-western section can also be used in estimating wave directions.

Although NL0 best estimates wave heights for the entire West Africa region from the West Africa grid simulation, NL1 produces better estimates for both south-eastern and north-western sub-divisions. In order to confidently determine which of these two non-linear source terms is to be used for projecting wave heights for the entire region, it is important to increase the number of observing stations, especially for the north-western sub-region, so as to reduce the errors in statistical estimations for much reliable comparisons to be made. So far, only one station represents the north-western sub-region of the study area because of the lack of available *in-situ* observed measurements. Concurrent *in-situ* measurement campaigns within the entire region are therefore recommended.

CRediT authorship contribution statement

Bennet Atsu Kwame Foli: Conceptualization, Methodology, Software, Validation, Formal analysis, Investigation, Writing – original draft, Data curation, Visualization, Project administration. **Joseph K. Ansong:** Conceptualization, Resources, Writing – review & editing, Visualization, Supervision. **Kwasi Appeaning Addo:** Conceptualization, Resources, Writing – review & editing, Visualization, Supervision. **George Wiafe:** Conceptualization, Resources, Writing – review & editing, Visualization, Supervision.

Declaration of Competing Interest

The authors declare that they have no known competing financial interests or personal relationships that could have appeared to influence the work reported in this paper.

Acknowledgments

We thank the Department of Marine and Fisheries Science of the University of Ghana, as well as the Regional Marine Centre at the University of Ghana for making buoy data from Ghana and Cabo Verde available. Thanks also to the International Marine and Dredging Consultants (IMDC) for making available ADCP data from Ghana. Thanks to Dr. Zacharie Sohou of IRHOB, Benin, for making buoy data from Benin available under the auspices of the GMES and Africa programme.

The wave model run computations was done using high performance computing (HPC) resources provided by the University of Ghana and the West African Centre for Cell Biology of Infectious Pathogens (WACCBIP) programme. Additional cloud computing and HPC resources was provided by the EU sponsored WEkEO Copernicus DIAS, and the Center for High Performance Computing (CHPC) in South Africa through the Weather, Climate and Water (ERTH0955) group of CHPC.

The study was supported by the Global Monitoring for Environment and Security and Africa (GMES & Africa) programme at the University of Ghana. Partial financial support was provided by the Open Society Foundation (OSF) under the Enhancing Efficiency and Effectiveness – Climate Change and Sustainability Development (EEE-CCSD) project. This study is part of the PhD. thesis of Bennet Atsu Kwame Foli.

We also thank the anonymous reviewers whose comments helped improve the manuscript.

References

Ardhuin, F., Herbers, T.H.C., O'Reilly, W.C., 2001. A hybrid eulerian–lagrangian model for spectral wave evolution with application to bottom friction on the continental shelf. J. Phys. Oceanogr. 31 (6), 1498–1516. https://doi.org/10.1175/1520-0485(2001)031.

Ardhuin, F., Rogers, E., Babanin, A.V., Filipot, J.-F.F., Magne, R., Roland, A.A.A., Van Der Westhuysen, A., Queffeulou, P., Lefevre, J.-M.M., Aouf, L., Collard, F., 2010. Semiempirical dissipation source functions for ocean waves. Part I: definition, calibration, and validation. J. Phys. Oceanogr. 40 (9), 1917–1941. https://doi.org/10.1175/2010JPO4324.1.

Auclair, J.-P., 2011. Implementation of the two-scale approximation in an operational wave model [Dalhousie University]. https://central.bac-lac.gc.ca/.item?id=TC-NSHD-14372&op=pdf&app=Library&oclc_number=871212503.

Booij, N., Haagsma, I.G., Holthuijsen, L.H., Kieftenburg, A.T.M.M., Ris, R.C., van der Westhuysen, A.J., Zijlema, M., 2004. SWAN Cycle III Version 40.41 Users Manual. Delft University of Technology, p. 118. https://swanmodel.sourceforge.io/download/zip/swanuse.pdf.

Booij, N., Ris, R.C., Holthuijsen, L.H., 1999. A third-generation wave model for coastal regions: 1. Model description and validation. J. Geophys. Res. Oceans 104 (C4), 7649–7666. https://doi.org/10.1029/98JC02622.

Chawla, A., Tolman, H., 2007. Automated grid generation for WAVEWATCH III. NWS Tech. Note 254, 1–77.

de León, S.P., Osborne, A.R., 2020. Role of nonlinear four-wave interactions source term on the spectral shape. J. Mar. Sci. Eng. 8 (4) https://doi.org/10.3390/jmse8040251.

Fernández, L., Calvino, C., Dias, F., 2021. Sensitivity analysis of wind input parametrizations in the WAVEWATCH III spectral wave model using the ST6 source term package for Ireland. Appl. Ocean Res. 115 (102826), 1–11. https://doi.org/10.1016/J.APOR.2021.102826.

Foli, B.A.K., Ansong, J.K., Appeaning Addo, K., Wiafe, G., 2022. A WAVEWATCH III® model approach to investigating ocean wave source terms for west africa: input-dissipation source terms. Remote Sens. Earth Syst. Sci. https://doi.org/10.1007/s41976-021-00065-y.

Foli, B.A.K., Appeaning-Addo, K., Ansong, J.K, Wiafe, G., 2021. Evaluation of ECMWF and NCEP reanalysis wind fields for long term historical analysis and ocean wave modelling in West Africa. Remote Sens. Earth Syst. Sci. https://doi.org/10.1007/s41976-021-00052-3.

Gouin, M., Ducrozet, G., Ferrant, P., 2016. Development and validation of a non-linear spectral model for water waves over variable depth. Eur. J. Mech. B/Fluids 57, 115–128. https://doi.org/10.1016/j.euromechflu.2015.12.004.

Gramstad, O., Babanin, A., 2016. The generalized kinetic equation as a model for the nonlinear transfer in third-generation wave models. Ocean. Dyn. 66, 509–526.

Hanna, S.R., Heinold, D.W., 1985. Development and Application of a Simple Method for Evaluating Air Quality Models, 4409th ed. American Petroleum Institute.

Hasselmann, K., 1960. Grundgleichungen der seegangsvoraussage. Schiffstechnik 1, 191–195.

Hasselmann, K., 1962. On the non-linear energy transfer in a gravity-wave spectrum: Part 1. General theory. J. Fluid Mech. 12 (4), 481–500. https://doi.org/10.1017/S0022112062000373.

Hasselmann, K., 1963a. On the non-linear transfer in a gravity wave spectrum, Part 2, conservation theory, wave-particle correspondence, irreversibility. J. Fluid Mech. 15, 273–281.

Hasselmann, K., 1963b. On the non-linear transfer in a gravity wave spectrum, Part 3. Evaluation of energy flux and sea-swell interactions for a Neuman spectrum. J. Fluid Mech. 15, 385–398.

Hasselmann, K., Barnett, T.P., Bouws, E., Carlson, H., Cartwright, D.E., Enke, K., Ewing, J.A., Gienapp, H., Hasselmann, D.E., Kruseman, P., Meerburg, A., Muller, P., Olbers, D.J., Richter, K., Sell, W., Walden, H., 1973. Measurement of wind-wave growth and swell decay during the Joint North Sea Wave Project (JONSWAP). Deutsch. Hydrogr. Inst. 12, 399–404.10.1038/nclimate1979%0Ahttps://doi.org/10.1016/j.coastaleng.2016.06.001%0Ahttp://www.e3s-conferences.org/10.1051/e3sconf/20160713014%0Ahttp://ascelibrary.org/doi/10.1061/%28ASCE%290733-9429%282005%29131%3A6%28497%29%0Ahttps://doi.org

Hasselmann, S., Hasselmann, K., 1985. Computations and parameterizations of the nonlinear energy transfer in a gravity-wave spectrum. Part I: a new method for efficient computations of the exact nonlinear transfer integral. J. Phys. Oceanogr. 15 (11), 1369–1377. https://doi.org/10.1175/1520-0485(1985)015<1369:CAPOTN>2.0.CO;2. Issue.

Hasselmann, S., Hasselmann, K., Allender, J.H., Barnett, T.P., 1985. Computations and Parameterizations of the nonlinear energy transfer in a gravity-wave specturm. part ii: parameterizations of the nonlinear energy transfer for application in wave models. J. Phys. Oceanogr. 15 (11), 1378–1391. https://doi.org/10.1175/1520-0485(1985)015<1378:CAPOTN>2.0.CO;2. Issue.

Herterich, K., Hasselmann, K., 1980. A similarity relation for the nonlinear energy transfer in a finite-depth gravity-wave spectrum. J. Fluid Mech. 97 (1), 215–224. https://doi.org/10.1017/S0022112080002522.

Holt, M., Cavaleri, L., Komen, G., Cavaleri, L., Donelan, M., Hasselmann, K., Hasselmann, S., Janssen, P., 1994. Wind interpolation. Dynamics and Modelling of Ocean Waves. Cambridge University Press, pp. 299–300. https://doi.org/10.1017/CBO9780511628955.

Kalourazi, M.Y., Siadatmousavi, S.M., Yeganeh-Bakhtiary, A., Jose, F., 2021. WAVEWATCH-III source terms evaluation for optimizing hurricane wave modeling: a case study of hurricane Ivan. Oceanologia 63 (2), 194–213. https://doi.org/10.1016/j.oceano.2020.12.001.

Khan, S.S., Echevarria, E.R., Hemer, M.A., 2021. Ocean swell comparisons between sentinel-1 and WAVEWATCH III around Australia. J. Geophys. Res. Oceans 126 (2), 1–23. https://doi.org/10.1029/2020JC016265.

Komatsu, K., Masuda, A., 1996. A new scheme of nonlinear energy transfer among wind waves: RIAM method-algorithm and performance. J. Oceanogr. 52, 509–537.

Liu, Q., Babanin, A., Fan, Y., Zieger, S., Guan, C., Moon, I.J., 2017. Numerical simulations of ocean surface waves under hurricane conditions: assessment of existing model performance. Ocean Modell. 118, 73–93. https://doi.org/10.1016/j.ocemod.2017.08.005.

Liu, Q., Rogers, W.E., Babanin, A.V., Young, I.R., Romero, L., Zieger, S., Qiao, F., Guan, C., 2019. Observation-based source terms in the third-generation wave model WAVEWATCH III: updates and verification. J. Phys. Oceanogr. 49 (2), 489–517. https://doi.org/10.1175/JPO-D-18-0137.1.

Mentaschi, L., Besio, G., Cassola, F., Mazzino, A., 2013. Problems in RMSE-based wave model validations. Ocean Modell. 72, 53–58. https://doi.org/10.1016/j.ocemod.2013.08.003.

Mentaschi, L., Besio, G., Cassola, F., Mazzino, A., 2015. Performance evaluation of Wavewatch III in the mediterranean sea. Ocean Modell. 90, 82–94. https://doi.org/10.1016/j.ocemod.2015.04.003.

Monbaliu, J., Hargreaves, J.C., Carretero, J.C., Gerritsen, H., Flather, R., 1999. Wave modelling in the PROMISE project. Coast. Eng. 37 (3–4), 379–407. https://doi.org/10.1016/S0378-3839(99)00035-6.

NOAA National Centers for Environmental Prediction, 2020. WAVEWATCH III® Production Hindcast, Multigrid: Feb 2005 to Mar 2019. NOAA National Centers for Environmental Prediction. https://polar.ncep.noaa.gov/waves/hindcasts/prod-multi_1.php.

Perrie, W., Toulany, B., Resio, D.T., Roland, A., Auclair, J.P., 2013. A two-scale approximation for wave-wave interactions in an operational wave model. Ocean Modell. 70, 38–51. https://doi.org/10.1016/j.ocemod.2013.06.008.

Perrie, W., Resio, D.T., 2009. A two-scale approximation for efficient representation of nonlinear energy transfers in a wind wave spectrum. Part II: application to observed wave spectra. J. Phys. Oceanogr. 39 (10), 2451–2476. https://doi.org/10.1175/2009JPO3947.1.

Polnikov, V., 2020. The fast discrete interaction approximation concept. Fluids 5 (4), 1–12. https://doi.org/10.3390/fluids5040176.

Puscasu, R.M., 2014. Integration of artificial neural networks into operational ocean wave prediction models for fast and accurate emulation of exact nonlinear interactions. Procedia Comput. Sci. 29, 1156–1170. https://doi.org/10.1016/j.procs.2014.05.104.

Remya, P.G., Rabi Ranjan, T., Sirisha, P., Harikumar, R., Balakrishnan Nair, T.M., 2020. Indian ocean wave forecasting system for wind waves: development and its validation. J. Oper. Oceanogr. 0 (0), 1–16. https://doi.org/10.1080/1755876X.2020.1771811.

Resio, D.T., Perrie, W., 1991. Numerical study of nonlinear energy fluxes due to wave–wave interactions. Part 1: methodology and basic results. J. Fluid Mech. 223, 603–629.

Resio, D.T., Perrie, W., 2008. A two-scale approximation for efficient representation of nonlinear energy transfers in a wind wave spectrum. Part I: theoretical development. J. Phys. Oceanogr. 38 (12), 2801–2816. https://doi.org/10.1175/2008JPO3713.1.

Resio, D.T., Pihl, J.H., Tracy, B.A., Vincent, C.L., 2001. Nonlinear energy fluxes and the finite depth equilibrium range in wave spectra. J. Geophys. Res. Oceans 106 (C4), 6985–7000. https://doi.org/10.1029/2000JC900153.

Swain, J., Umesh, P.A., J, S., PA, U., 2018. Prediction of uncertainty using the third generation wave model WAVEWATCH III driven By ERA-40 and blended winds in the North Indian ocean. J. Oceanogr. Mar. Res. 06 (01), 1–17. https://doi.org/10.4172/2572-3103.1000173.

Swain, J., Umesh, P., Balchand, A., 2019. WAM and WAVEWATCH-III intercomparison studies in the North Indian ocean using oceansat-2 scatterometer winds. J. Ocean Clim. Sci. Technol. Impacts 9, 1–24. https://doi.org/10.1177/2516019219866569.

Tamura, H., Waseda, T., Miyazawa, Y., Komatsu, K., 2008. Current-induced modulation of the ocean wave spectrum and the role of nonlinear energy transfer. J. Phys. Oceanogr. 38 (12), 2662–2684. https://doi.org/10.1175/2008JPO4000.1.

Tolman Hendrik L., 2010. State of the art of wave modeling. 57. http://polar.ncep.noaa.gov/waves/workshop/pdfs/wwws_2.1.pdf.

Tolman, H., Krasnopolsky, V., 2004. Nonlinear interactions in practical wind wave models. In: Proceedings of the 8Th International Workshop on Wave. ftp://www.wmo.int/Documents/PublicWeb/amp/mmop/documents/JCOMM-TR/J-TR-29-WH8/Papers/E1.pdf.

Tolman, H.L., 1991. A third-generation model for wind waves on slowly varying, unsteady, and inhomogeneous depths and currents. J. Phys. Oceanogr. 21, 782–797.

Tolman, H.L., 2002. Alleviating the garden sprinkler effect in wind wave models. Ocean Modell. 4 (3–4), 269–289. https://doi.org/10.1016/S1463-5003(02)00004-5.

Tolman, H.L., 2004. Inverse modeling of discrete interaction approximations for nonlinear interactions in wind waves. Ocean Modell. 6 (3–4), 405–422. https://doi.org/10.1016/j.ocemod.2003.09.002.

Tolman, H.L., 2013. A generalized multiple discrete interaction approximation for resonant four-wave interactions in wind wave models. Ocean Modell. 70, 11–24. https://doi.org/10.1016/j.ocemod.2013.02.005.

Tolman, H.L., Balasubramaniyan, B., Burroughs, L.D., Chalikov, D.V., Chao, Y.Y., Chen, H.S., Gerald, V.M., 2002. Development and implementation of wind-generated ocean surface wave models at NCEP. Weather Forecast. 17 (2), 311–333. https://doi.org/10.1175/1520-0434(2002)017<0311:DAIOWG>2.0.CO;2.

Tolman, H.L., Chalikov, D., 1996. Source terms in a third-generation wind wave model. J. Phys. Oceanogr. 26 (11), 2497–2518. https://doi.org/10.1175/1520-0485(1996)026<2497:STIATG>2.0.CO;2. Issue.

Tolman, HL., Grumbine, R.W., 2013. Holistic genetic optimization of a generalized multiple discrete interaction approximation for wind waves. Ocean Modell. 70, 25–37. https://doi.org/10.1016/j.ocemod.2012.12.008.

Tracy, B., & Resio, T., 1982. Theory and calculation of the nonlinear energy transfer between sea waves in deep water.

van Vledder, G., 2002. Improved parameterisations of nonlinear four wave interactions for application in operational wave prediction models. August. doi:10.13140/RG.2.2.17044.50564.

van Vledder, G.P.h., 2012. Efficient algorithms for non-linear four-wave interactions. ECMWF Workshop on Ocean Waves, June, 97–112. http://resolver.tudelft.nl/uuid:c88a7808-e991-4e7a-b667-8c4074149c3b.

van Vledder, G.P.h., 2006. The WRT method for the computation of non-linear four-wave interactions in discrete spectral wave models. Coast. Eng. 53 (2–3), 223–242. https://doi.org/10.1016/j.coastaleng.2005.10.011.

WAMDI Group, 1988. The WAM model—a third generation ocean wave prediction model. J. Phys. Oceanogr. 18 (12), 1775–1810. https://doi.org/10.1175/1520-0485(1988)018<1775:TWMTGO>2.0.CO;2.

Wang, J., Zhang, J., Yang, J., Bao, W., Wu, G., Ren, Q., 2017. An evaluation of input/dissipation terms in WAVEWATCH III using in situ and satellite significant wave height data in the South China Sea. Acta Oceanol. Sin. 36 (3), 20–25. https://doi.org/10.1007/s13131-017-1038-7.

van Vledder, G.P.h., & Bottema, M., 2003. Improved modelling of nonlinear four-wave interactions in shallow water. September 2014, 459–472. doi:10.1142/9789812791306_0040.

WAVEWATCH III Development Group, 2016. User manual and system documentation of WAVEWATCH III version 5.16 (Tech. Note). NOAA/NWS/NCEP/MMAB.

Webb, D.J., 1978. Non-linear transfers between sea waves. Deep-Sea Res. 25, 279–298.

Young, I.R., Van Vledder, G.P., 1993. A review of the central role of nonlinear interactions in wind-wave evolution. Philos. Trans. Phys. Sci. Eng. 342 (1666), 505–524. https://www.jstor.org/stable/54171.